

Evaluation of surface preparation methods for glass

N. P. Mellott,^{1*} S. L. Brantley,² J. P. Hamilton^{1†} and C. G. Pantano¹

¹ Department of Materials Science and Engineering, The Pennsylvania State University, University Park, PA 16802, USA

² Department of Geosciences, The Pennsylvania State University, University Park, PA 16802, USA

Received 16 August 2000; Revised 22 November 2000; Accepted 28 November 2000

In this study, methods of surface preparation by polishing, fiber-drawing, melt-casting and chemical etching were evaluated with x-ray photoelectron spectroscopy (XPS) and atomic force microscopy (AFM) for a variety of alkali and alkaline earth aluminosilicate glasses. Freshly polished glass surfaces were exposed to a variety of chemical etchants (NaOH, NH₄OH and HF) and the resulting surface composition and morphology are reported. The polishing and etching parameters were optimized to obtain a smooth surface (root-mean-square (RMS) roughness of ≤ 3 nm) and a surface composition as close as possible to the bulk composition. In addition, glass melt and fiber surfaces were examined to investigate the effect of thermal processes on surface composition and morphology. It is shown that polishing can alter the surface composition of these multicomponent glasses, and that post-etching of the polished surface to expose the bulk composition is plagued by preferential leaching, contamination and/or roughening. The most significant conclusion is that there is a strong dependence of these surface compositional modifications upon the specific glass; even within specific glass systems, the polish/etch procedure must be modified to yield a surface with the bulk composition. On the other hand, the smoothness of fibers and melt-cast surfaces is ideally suited to AFM and depth profiling; their surface compositions can be close to the bulk values, but careful attention to the annealing conditions is required to achieve this. Copyright © 2001 John Wiley & Sons, Ltd.

KEYWORDS: glass; polishing; XPS; AFM; surface composition

INTRODUCTION

Many technological applications of glass depend upon the quality of the surface. This is especially true in the new and emerging applications of glass for displays,¹ microelectronics² and advanced lithography.³ In addition, clean, smooth, compositionally reproducible sample surfaces are desirable for various surface science studies of materials, e.g. corrosion, adsorption, film deposition, etc. In most glassmaking processes, thermal and chemical effects directly influence the final composition, morphology, defect density and durability of a glass surface. For example, the annealing of some glass compositions can deplete or enrich the surface in metal ions if they are susceptible to evaporation or segregation. In the case of glass fibers, flame-assisted fiberization⁴ or aging of some fiber compositions⁵ can alter the surface composition relative to the bulk.

In the chemical–mechanical polishing and/or aqueous-based cleaning of glass, a thin leached surface layer is often observed to form. A recent symposium on the finishing of advanced ceramics and glasses provides a timely review of these issues.⁶ In particular, Cook and others have

investigated the chemical effects involved in the polishing of silicate glasses.^{7–11} Cook reports that at the expected length-scale for glass/slurry interactions (molecular) the rate of material removal from the glass surface is controlled by a combination of the following processes: molecular water diffusion into the glass surface, glass dissolution, adsorption rate of dissolution products onto the polishing agent, silica redeposition onto the glass surface and the aqueous corrosion rate of the bulk glass.

Atomic force microscopy (AFM) has been used extensively for quantification of the surface microtopography of various types of surfaces. The root-mean-squared (RMS) roughness is commonly used to quantify micro- and nanoscale surface roughness.^{12–15} It has been applied to examine the effect of polishing on minerals and mineral-based ceramics,^{15–19} fused silica^{14,15} and silicon nitride.¹⁸ The reported RMS roughness values for ‘optically polished’ silica, multicomponent silicate glasses and glass-ceramics fall in the range of 0.1–1.5 nm; examples of reported RMS roughness values of common silicate glasses as a function of polishing procedures are compiled in Table 1.

After polishing, it is common to employ an acid or base etch to eliminate the damaged/compositionally modified (silica-rich) layer formed on the glass surface. Carre, *et al.*²⁰ used electrostatic measurements of the point of zero charge to conclude that HCl treatment of ground, abraded or fire-polished glass produces surfaces whose compositions

*Correspondence to: N. P. Mellott, The Pennsylvania State University, 103 Materials Research Institute, University Park, PA 16802, USA. E-mail: npm113@psu.edu

†Present address: Johns Manville Technical Center, Littleton, CO 80162, USA.

Contract/grant sponsor: Department of Energy; Contract/grant number: DE-FG02-95ER14547.A000.

Table 1. Measured RMS roughness, by AFM, of some common commercial glasses

Glass	Surface	RMS (nm)	Ref.
Zerodur	Optical polish	≤0.1	15
Zerodur	Float polish	~0.3	14
Fused silica	Optical polish	~0.1–0.2	15
Fused quartz	Float polish	~0.2	14
ULE	Float polish	~0.5	14
BK7	Optical polish	~0.2–0.4	15
BK7	Commercial polish	~1.2	12
Soda lime	Fire polish	~0.3	13
Soda lime	Fire polish	~0.1	13
BPSG	CVD	~1.4	1
BPSG	CVD	~0.2	1

reflect the bulk composition. This, however, can exert a negative impact on the surface roughness. Experimentally, it has been reported that KOH etching (15 min) of fire-polished soda-lime silicate glass results in an RMS roughness increase of a factor of two (from 0.3 to 0.7 nm), as measured by AFM.¹³ In the case of polished fused silica, dilute HF etching changes the surface RMS roughness from ~0.8 nm to ~2.3 nm (with an etched depth of 10 μm).¹⁹ Usually, this roughness increase can be associated with the re-appearance of polishing grooves.

Although these investigations report the effects of finishing glass in terms of the surface topography and RMS surface roughness, the corresponding effect on surface composition has not been studied. In this study, XPS has been used to determine the extent to which the surface composition is modified with various polishing and etching conditions; AFM is used to characterize the corresponding effects on RMS roughness. The rationale for the study of etching is to find a procedure whereby the surface can be congruently dissolved (or stripped) to create a compositionally 'bulk' surface. Subsequently, the characteristics of these polished/etched surfaces are compared with those of frozen-melt surfaces. The use of polishing and etching to create reproducibly smooth surfaces with the bulk composition is discussed relative to frozen-melt surface preparation by casting or fiber-drawing.

EXPERIMENTAL

Glass melting

Raw materials for the melting of glasses included Min-U-Sil SiO₂, reagent-grade Al(OH)₃, reagent-grade CaO, anhydrous Na₂CO₃ and Na₂SO₄ powders. Batches of each composition were melted in platinum crucibles for 16–24 h at temperatures ranging from 1400 to 1750 °C in air and were poured into graphite molds to form either rods or plates. The rods and plates were then annealed overnight at temperatures ranging from 500 to 750 °C and cooled slowly to room temperature. Spectrochemical analyses (based on a lithium metaborate fusion process followed by inductively coupled plasma atomic emissions spectroscopy (ICPAES) analysis of the resulting solution) and/or electron probe

Table 2. Glass compositions

Sample	Mol%				At.%				
	SiO ₂	Al ₂ O ₃	CaO	Na ₂ O	Si	Al	Ca	Na	O
NAS0.8	55	20	—	25	16	12	—	15	57
NAS0.6	60	15	—	25	18	9	—	15	58
NAS0.4	65	10	—	25	20	7	—	16	58
NAS0.2	70	5	—	25	23	3	—	16	58
NAS0.0	75	0	—	25	25	0	—	16	59
NAS112	50	25	—	25	14	14	—	14	58
CAS112	50	25	25	—	15	15	8	—	62
Ca20	56	22	19	3	17	13	6	2	62
Ca15	60	20	15	5	19	12	5	3	62
Ca10	62	20	9	9	19	12	3	5	61
CAS1509	60	14	26	—	22	6	10	—	62

microanalysis (EPMA) of the glasses indicated only minor deviation from their batch compositions; Table 2 reports the batch compositions.

Glass-surface preparation (polishing and etching)

The glass plates were cut with a 5 inch Buehler diamond saw blade (0.25 inch thickness) to 2 cm × 1 cm × 0.2 cm. Samples were then ground with 240, 400 and 600 grit silicon carbide grinding pads. Following grinding, samples were mounted on a polishing disk (capacity of eight samples per disk) and rough polished using 6 μm (20 min), 3 μm (10 min), 1 μm (10 min), 0.25 μm (10 min) and 0.1 μm (15 min) oil-based diamond sprays, using a LECO AP-60 automatic polisher. Between each grit change, the samples were thoroughly rinsed with acetone and wiped gently. After the final polish (0.1 μm), samples were cleaned ultrasonically for 15 min in spectroscopic-grade acetone followed by 30 min of ultraviolet ozone cleaning (UVOC).

The polished NAS 0.8 and CAS112 samples were etched in a variety of solutions in an attempt to find a method that would yield a clean, smooth glass surface with a surface composition as close to the bulk composition as possible. Table 3 is a summary of the etchants evaluated (1 N NaOH at 80 °C for 3 min, 48% HF at 80 °C for 1 s, 4% HF at 80 °C for 5 min, 1 N NH₄OH at 80 °C for 3 min and 1 N NH₄OH at 80 °C for 30 min). In some cases, an acid rinse (1 N acetic acid) was evaluated for removing residue of the concentrated etch solution. Following etching and/or

Table 3. Etching techniques

Etchant	Rinse	Etch time (s)	Temperature (°C)
NaOH(1 N)	RO water	180	80
NaOH(1 N)	Acetic acid, RO water	180	80
HF (100%)	RO water	1	25
HF (4%)	RO water	10	25
HF (1%)	RO water	5	25
NH ₄ OH	RO water	180	80
NH ₄ OH	Acetic acid, RO water	180	80

RO = Reverse Osmosis-filtered.

acidic rinsing the samples were immediately rinsed in RO water at 80 °C and blown dry with nitrogen gas. Immediately before all surface analyses, the samples were cleaned by ultraviolet ozone cleaning (UVOC) for 30 min to remove residual hydrocarbons.

Once polishing and etching techniques were optimized for NAS 0.8 and CAS112 (based on XPS analysis of surfaces whose composition most closely resembled the bulk), the composition dependence was evaluated using the glasses listed in Table 2.

Glass-surface preparation (melt and fiber surfaces)

The CAS1509 and CAS112 glasses were re-melted in a platinum crucible at 1650 °C for 3 h. The melts were poured into buttons (~25 mm in diameter) on a graphite plate. The CAS1509 buttons were produced with three different thermal histories: unannealed; annealed at 780 °C for 1 h and cooled at a rate of 1 °C min⁻¹ for 7 h; and annealed at 780 °C for 3 h and cooled at a rate of 3 °C min⁻¹ for 7 h. The CAS112 buttons were annealed at 650 °C for 12 h and cooled at 1 °C min⁻¹ for 10 hours. Once removed from the annealing furnace, the samples were immediately stored in a vacuum desiccator until the time of surface analyses.

The CAS fibers (~10 µm diameter) were drawn through a single-tip bushing using glass culet that had been homogenized by repeated melting and crushing.⁵

X-Ray photoelectron spectroscopy

The surface compositions (outermost ~80 Å) of all samples were analyzed with a Kratos XSAM 800 spectrometer. The XPS analyses were collected with Mg K α x-rays (non-monochromatic) at 20 mA anode current, with an electron accelerating voltage of 14 kV, a pass energy of 80 eV and a step size of ~0.1 eV. The collection time for each peak was adjusted to yield a signal-to-noise ratio of >50:1. The analyzed area was ~2–3 mm in diameter.

Quantitative surface compositions were determined for all samples from high-resolution scans of the Na KLL, O 1s, Si 2p, Ca 2p and Al 2p peaks. Sensitivity factors of all elements were derived from fresh air-fracture surfaces of CAS112 (Ca, Si and Al), Ca15 (Ca, Na, Si and Al) and NAS112 (Na, Si and Al), assuming that the fracture surface was identical to the bulk composition (for these samples, the bulk compositions were determined independently from EMPAs). The matrices of all glasses are similar, so the compositions reported here correspond to the *average* composition over the outermost 80 Å of the surface.

Atomic force microscopy

Glass surfaces were imaged with a Digital Instruments Nanoscope IIIa Dimension 3100 atomic force microscope. Both height and amplitude images were collected in Tapping Mode[®], with a sharpened tip, at a scan rate of 1.0 Hz. All probes used were commercially available Tapping Mode etched silicon probes (TESP) with a nominal tip radius of 5–10 nm, a cantilever length of 125 µm, and a resonance frequency of ~200–400 Hz. For all high-resolution scans (≤ 1 µm), tips were evaluated further using a gold and/or tin oxide standard to ensure tip radii of <10 nm. Multiple

scans were taken of each sample at different locations on the surface to ensure a large-scale spatial averaging of roughness. Ten 1 µm × 1 µm areas of each sample were then imaged for analysis. The resolution of each image is determined by the scan size; for this reason, comparisons of roughness between samples reported in various parts of this study were determined using images of equal resolution.

The RMS roughness calculations were performed with Digital Instrument software.²¹ Flattening and third-order plane fitting were performed on each image prior to analysis, to remove any tip artifacts caused by the curvature of the piezoelectric material, thermal drift or lateral forces.²² Flattening removes vertical offsets between scan lines through calculation of a least-squares polynomial fit for a scan line and subtraction of the polynomial fit from the original line. Third-order plane fitting calculates a third-order polynomial fit to the image in the *x*- and *y*-directions and subtracts the polynomial fit from the image, removing tilt and S-shaped bow.^{21,22}

Root-mean-square roughness (*RMS*) is defined as the root-mean-square average of height deviations from the mean elevation plane, calculated from the relative heights of each pixel in the image

$$RMS = \sqrt{((z_1^2 + z_2^2 + \dots + z_N^2)/N)} \quad (1)$$

where z_i equals the difference in height from the mean plane for each point i and N equals the number of points measured.

RESULTS AND DISCUSSION

Surface composition

NAS glasses

All polished/unetched and polished/etched surfaces of NAS0.8 glass were found to be depleted in Na and Al (with respect to the bulk 'fracture' surface). This can be seen in the data of Fig. 1 by comparing the XPS concentration ratios for the finished surfaces to that of the bulk (fracture surface). It is somewhat surprising that the final Na surface concentration

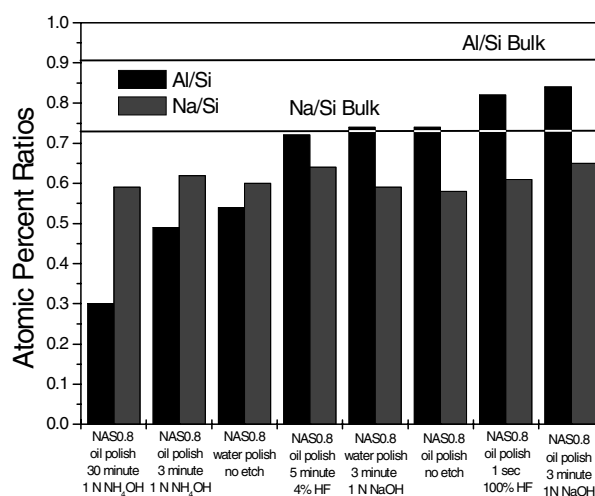


Figure 1. Sodium and aluminum to silicon ratios (by XPS) of various etching techniques on NAS 0.8 glass polished to 0.1 µm with diamond sprays.

is insensitive to the nature of the polishing slurry (water vs. oil) or the use of a post-etch. On the other hand, the final Al concentration at the surface varied substantially with the finishing process. The polishing process creates an Al-depleted silica-rich surface layer that is most evident for the water polish and less evident in the case of the oil polish. This Al-depleted layer is eliminated after etching in HF or NaOH, but not by etching in NH_4OH .

In general, NH_4OH was the least effective etchant, as exhibited by low Al/Si (and Na/Si) ratios compared with the fracture surfaces. Although the concentrated HF was effective in creating a surface without the Al depletion, a significant amount of F was strongly adsorbed ($\text{F/Si} = 0.51$); less F was adsorbed to the surface ($\text{F/Si} = 0.12$) with the dilute HF (4%). The most effective etchant was NaOH at 80°C for 3 min; it provided a surface composition that most nearly matched the fracture surface composition.

The complete series of Na–Al–Si glasses (NAS0.0, NAS0.2, NAS0.4, NAS0.6 and NAS0.8) were subjected to an oil polish followed by a 3 min etch in 1 N NaOH at 80°C . The data in Fig. 2 show that, in general, this polishing/etch treatment always leaves a somewhat compositionally modified surface. The treatment works best for NAS0.6 and NAS0.8, but when the Al_2O_3 content of the glass falls below 15 mol.% (NAS0.6) there is extensive surface depletion of Na. This clearly implies a composition dependence to the polishing and etching of glass when a surface with the bulk composition is required.

CAS glasses

All polished/unetched and polished/etched surfaces of the CAS112 glass were found to be depleted of Ca and Al. These data are summarized in Fig. 3. In this system, the depletion of Ca and Al is rather dramatic due to the oil polish alone. Here, too, the use of HF to strip the leached layer from the polished surface was plagued by F contamination. The 1 N NaOH etch was not very effective in eliminating the silica-rich surface layer and, in addition, contaminated the surface with Na ($\text{Na/Si} = 0.08$). With the addition of an acetic acid rinse after

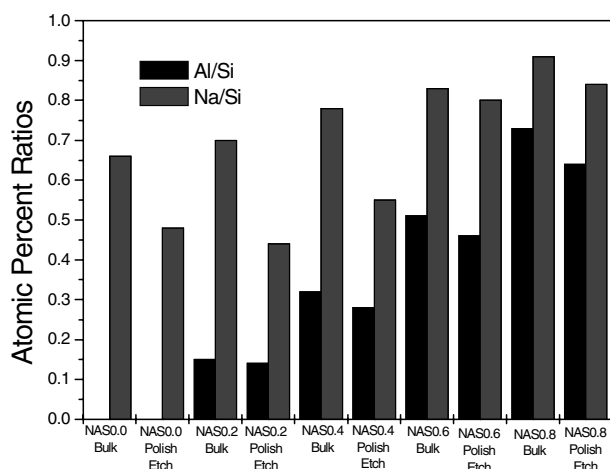


Figure 2. Sodium and aluminum to silicon ratios (by XPS) of various sodium aluminosilicate glasses polished to $0.1\ \mu\text{m}$ with diamond sprays, etched for 3 min at 80°C in 1 N NaOH, rinsed for 3 min at 80°C and UVOC for 30 min.

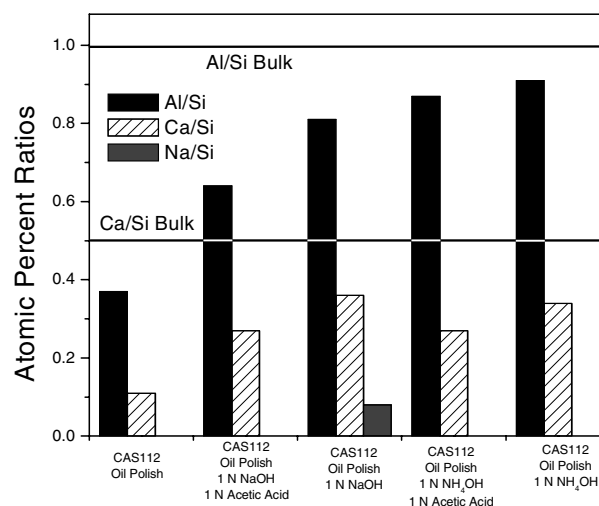


Figure 3. Calcium and aluminum to silicon ratios (by XPS) of various etching techniques on CAS112 glass polished to $0.1\ \mu\text{m}$ with diamond sprays.

the 1 N NaOH etch, the residual Na is removed but the Ca and Al were further depleted. The most effective etchant was NH_4OH because it provided a surface composition (Ca/Si and Al/Si ratio) that most nearly matched the bulk composition and it did not leave any residual contaminants (including NH species) on the surface.

The oil polish followed by the NH_4OH etch was applied to CAS112, NAS112 and aluminosilicate glasses with both Na and Ca (Ca10, Ca15 and Ca20). In all cases, the surface compositions of the finished (polished/etched) glasses did not equal the bulk composition. Interestingly, the depletion of Ca was accompanied by an enrichment of Na in two of the three mixed Na–Ca (Ca15 and Ca20) glasses. These data further verify the composition dependence of polishing/etching on the glass surface composition, and lead to the important conclusion that a single polishing/etching treatment will not be perfect (even within the family of aluminosilicate glasses). Clearly, the fact that the NAS0.8 (in Fig. 2) and CAS112 (in Fig. 4) possess the most bulk-like surface compositions is due to the fact that the polishing/etching treatments were optimized with these glasses.

Melt surfaces

Figure 5 shows the effect of casting, annealing and fiber-drawing on the surface composition of two Ca–Al–Si glasses. The surface composition of the unannealed CAS1509 melt surface was slightly enriched in Al and depleted in Ca with respect to the bulk composition, but after annealing this surface exhibits a composition only slightly depleted in Al and Ca. The corresponding CAS1509 fiber surface was also slightly depleted in Al, but was somewhat enriched in Ca. The CAS112 melt surface composition was also depleted slightly in Al and Ca. Altogether, Fig. 5 reveals that annealed melt surfaces can be prepared with compositions closer to the bulk than polished/etched surfaces.

Root-mean-square surface roughness

The AFM imaging of polished, unetched CAS1509 and CAS112 glass plates shows surfaces with numerous polishing

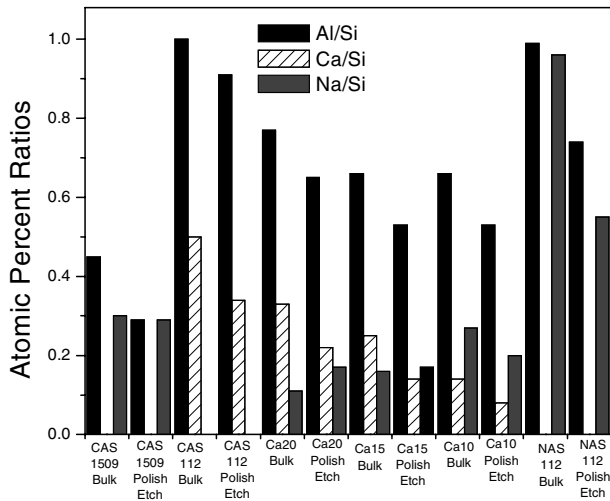


Figure 4. Calcium, sodium and aluminum to silicon ratios (by XPS) of various alkali and alkaline earth aluminosilicate glasses polished to 0.1 μm with diamond sprays, etched for 3 min at 80 °C in 1 N NH₄OH, rinsed for 3 min at 80 °C and UVOC for 30 min.

grooves. After etching, the surface features are more rounded and smoothed but, nevertheless, polishing grooves are

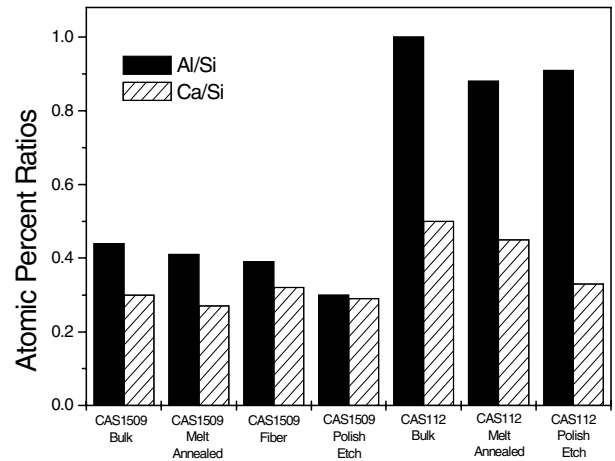
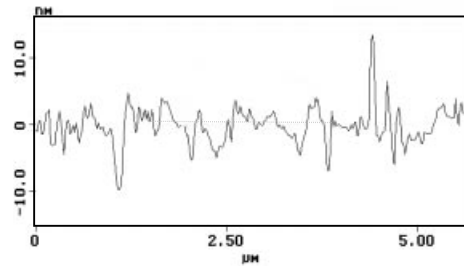
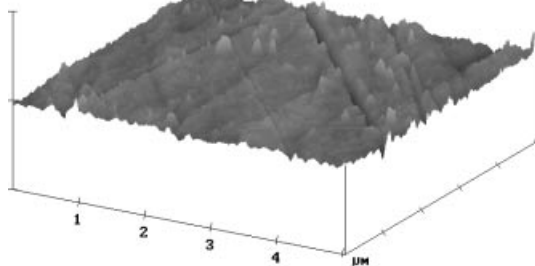


Figure 5. Calcium and aluminum to silicon ratios of bulk, melt, polished/etched and fiber surfaces of CAS1509 and CAS112.

still evident. Some AFM images of polished/unetched and polished/etched surfaces are shown in Fig. 6. The AFM imaging of more than 25 separate areas on a given polished surface and RMS analysis of about ten 1 μm × 1 μm areas of each surface revealed a wide range of polishing-induced surface features (i.e. the density, width and depth of

CAS1509 Polished Plate (Unetched)
RMS = 3.46 ± 0.55



CAS1509 Polished Plate (3 minute; 1 N NH₄OH Etch)
RMS = 3.35 ± 0.30

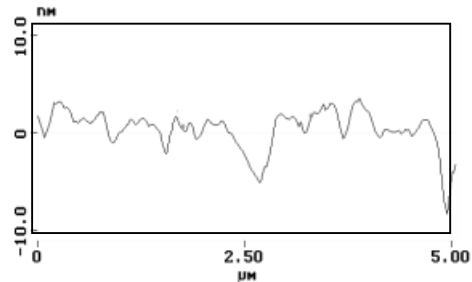
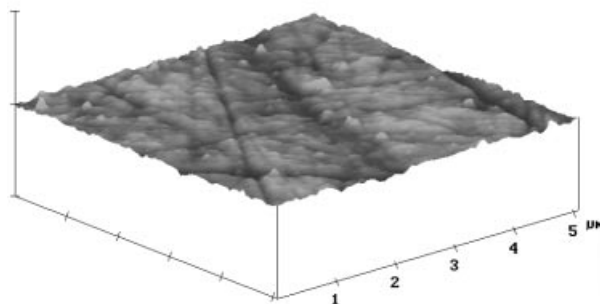


Figure 6. Representative AFM (height) images and cross-sections of CAS polished/unetched and CAS polished/etched surfaces. The x- and y-scales on both images are 5 μm × 5 μm, with a z-range of 100 nm. The x- and y-scales on both cross-sections are 5 μm, with a z-scale of 10 nm.

polishing scratches). This leads to a wide range of measured RMS roughness, not only from sample to sample but for different analysis spots on one sample. The error reported for RMS roughness values in Table 4 represents the standard deviation of the measured roughness divided by the square root of the number of scans (≥ 10).

The RMS roughnesses of polished CAS1509 and CAS112 are 3.46 ± 0.55 and 3.64 ± 0.54 nm, respectively (Table 4). After etching in 1 N NH_4OH , the RMS roughnesses of these surfaces are 3.35 ± 0.30 and 4.42 ± 0.32 nm, respectively (Table 4). These numbers are consistent with the AFM images wherein the unetched surface roughness is propagated, not eliminated, by the etch (Fig. 6).

The AFM imaging of the CAS1509 melt and fiber surfaces revealed a smoother, more spatially homogeneous surface topography than for the polished/*etched* surfaces. Representative AFM images of the CAS1509 melt and fiber surfaces are shown in Fig. 7. In general, the cast and fiber surfaces are 10–20 times smoother than the polished/*etched* surfaces. Moreover, the surfaces are consistently more homogeneous (with respect to roughness). The AFM imaging

Table 4. RMS roughness of CAS and CAS112

Sample	Surface-type	RMS	σ
CAS1509	polished unetched	3.46	0.55
CAS1509	polished etched	3.35	0.30
CAS1509	fiber	0.26	0.07
CAS1509	melt ¹	0.29	0.04
CAS1509	melt ²	0.26	0.01
CAS1509	melt ³	0.17	0.01
CAS112	polished unetched	3.64	0.54
CAS112	polished etched	4.42	0.32
CAS112	melt ⁴	0.25	0.01

¹ Unannealed.

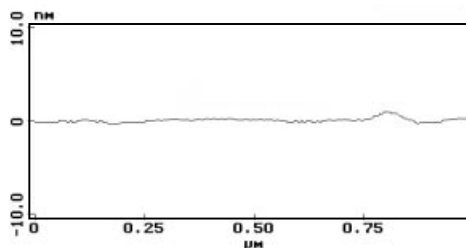
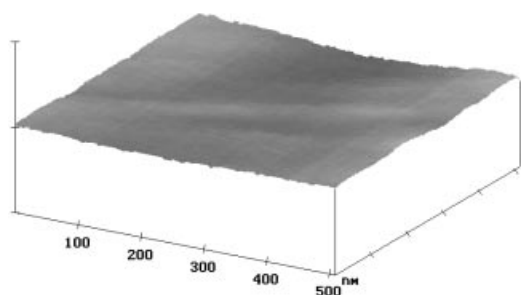
² Annealed at 780 °C 1 hr and cooled 1 °C/min.

³ Annealed at 780 °C 3 hr and cooled 3 °C/min.

⁴ Annealed at 650 °C 12 hr and cooled 1 °C/min.

of more than 25 separate areas on a given melt and/or fiber surface and RMS analysis of about ten $1 \mu\text{m} \times 1 \mu\text{m}$ areas of each surface revealed that roughness values

CAS1509 Glass Fiber RMS = 0.26 ± 0.07



CAS1509 Melt Surface RMS = 0.17 ± 0.01

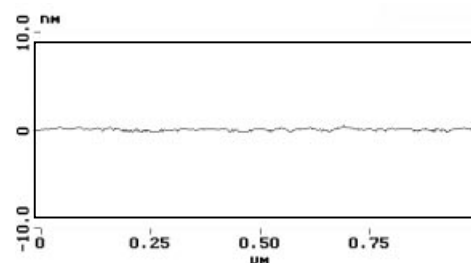
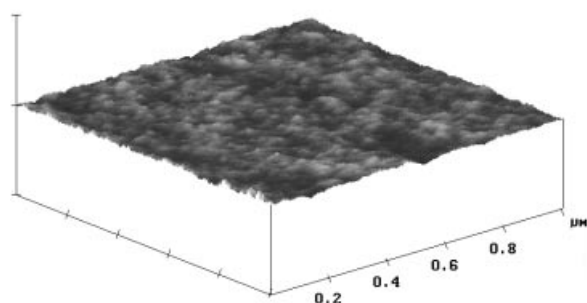


Figure 7. Representative AFM (height) images and cross-sections of CAS1509 fiber and CAS1509 melt surfaces. The x- and y-scales on both images are $500 \text{ nm} \times 500 \text{ nm}$, with a z-range of 10 nm. The x- and y-scales on both cross-sections are 500 nm , with a z-scale of 10 nm.

varied little regardless of where on the surface the RMS measurement was made. This homogeneity is reflected in the standard deviations reported with the RMS values (Fig. 6 and Table 4).

CONCLUSIONS

We have shown that multicomponent aluminosilicate glasses, in general, undergo significant surface composition changes during polishing (even in non-aqueous media). This polishing-induced surface modification often leaves a silica-rich surface layer. This is in contrast to the suggestions of Carre *et al.*,²⁰ who concluded that abrasion and grinding of glass leaves a more alkaline surface; their conclusions, however, were based on the point of zero charge and not direct compositional analysis. A post-etch can be used to strip the polishing-induced surface layer and create a smooth surface with the bulk composition provided that the etch does not further leach, roughen or contaminate the surface. The ability of an etch (HF, NaOH, NH₄OH) to achieve this depends upon the specific glass. This suggests that: the solubility and microstructure of the silica-rich leached layers vary from glass to glass: some leaching and/or incongruent dissolution occurs, even in HF, NaOH and/or NH₄OH; and adsorption (e.g. F⁻ or NH₄⁺) or ion exchange (e.g. Na⁺ for Ca²⁺) can occur to varying degrees during etching in HF, NaOH or NH₄OH. Altogether, we conclude that the optimal polishing and etching treatment necessary to achieve a bulk-like surface composition varies with the bulk glass composition, even within the aluminosilicate glass family.

The RMS roughnesses of polished surfaces prepared in this study were of the order of 3–4 nm, through the use of more sophisticated finishing methods this can be 20 times better, but in all cases the surface compositions, at least for multicomponent aluminosilicate glass, will be modified. Conversely, melt surfaces can be fabricated that have a uniform 0.2 nm RMS roughness and that possess a surface composition close to that of the bulk. Thus, in those cases where cast or fiberized frozen-melt surfaces can be used, the ability to control and study intrinsic surface reactions of glass will be improved.

Acknowledgements

The authors would like to thank Jeff Shallenberger, ChangQing Shen and Vince Bojan for helpful advice and technical hints. Funding for this work was supported by the Department of Energy, Office of Basic Energy Sciences, Grant DE-FG02-95ER14547.A000.

REFERENCES

1. Bocko PL, Fenn PM, Morse LR, Okamoto F. *SID 91 Dig.* 1991; 675.
2. Tang SK, Vassiliev VY, Mridha S, Chan LH. *Thin Solid Films* 1999; **352**: 77.
3. Tong WM, Taylor JS, Vernon SP. In *Finishing of Advanced Ceramics and Glasses*, vol 102. Sabia R, Greenhut VA, Pantano CG (eds). The American Ceramic Society: Westerville, 1999; 233–243.
4. Palmisiano MN, Boehman AL, Pantano CG. *J. Am. Ceram. Soc.* 2000; **10**: 2423.
5. Pantano CG. *Rev. Solid State Sci.* 1989; **3**: 379.
6. Sabia R, Greenhut VA, Pantano CG. *Finishing of Advanced Ceramics and Glasses*, vol 102. The American Ceramic Society: Westerville, 1999; 365.
7. Cook LM. *J. Non-Cryst. Solids* 1990; **120**: 152.
8. Cook LM, Mader KH. *Glastech. Ber.* 1987; **7**: 234.
9. Cook LM, Marker AJ, Mader KH, Muller H. *Glastech. Ber.* 1987; **9**: 302.
10. Cook LM, Mader KH. *Glastech. Ber.* 1987; **10**: 333.
11. Dunken H. *J. Non-Cryst. Solids* 1991; **129**: 64.
12. Meyer E, Haefka H, Guntherod HJ, Anderson O, Bange K. *Glastech. Ber.* 1993; **66**: 30.
13. Radlein E, Frischat GH. *J. Non-Cryst. Solids* 1997; **222**: 69.
14. Bennett JM, Shaffer JJ, Shibano Y, Namba Y. *Appl. Opt.* 1987; **26**: 696.
15. Bennett JM, Jahanmir J, Podlensky JC, Balter TL, Hobbs DT. *Appl. Opt.* 1995; **34**: 213.
16. Sabia R, Stevens HJ, Varner JR. *J. Non-Cryst. Solids* 1999; **249**: 123.
17. Dickinson JT, Hariadi RF, Langfor SC. In *Finishing of Advanced Ceramics and Glasses*, vol 102. Sabia R, Greenhut VA, Pantano CG (eds). The American Ceramic Society: Westerville, 1999; 213–232.
18. Muratov VA, Fisher TE. In *Finishing of Advanced Ceramics and Glasses*, vol 102. Sabia R, Greenhut VA, Pantano CG (eds). The American Ceramic Society: Westerville, 1999; 245–258.
19. Carr JW, Fearson E, Summers LJ, Hutcheon ID, Haack JK, Hoskins S. In *Finishing of Advanced Ceramics and Glasses*, vol 102. Sabia R, Greenhut VA, Pantano CG (eds). The American Ceramic Society: Westerville, 1999; 163–175.
20. Carree A, Roger F, Varinot C. *J. Coll. Interface Sci.* 1992; **154**: 174.
21. Digital Instruments. *Command Reference Manual*, 1997.
22. Ruppe C, Duparee R. *Thin Solid Films* 1996; **288**: 8.